Hydrol. Earth Syst. Sci., 20, 4857–4865, 2016
www.hydrol-earth-syst-sci.net/20/4857/2016/
doi:10.5194/hess-20-4857-2016

Hydrology and Earth System Sciences
Open Access
EGU

Matching the Budyko functions with the complementary evaporation relationship: consequences for the drying power of the air and the Priestley–Taylor coefficient

Jean-Paul Lhomme[1] **and Roger Moussa**[2]

[1]IRD, UMR LISAH, 2 Place Viala, 34060 Montpellier, France
[2]INRA, UMR LISAH, 2 Place Viala, 34060 Montpellier, France

Correspondence to: Roger Moussa (roger.moussa@inra.fr)

Received: 10 May 2016 – Published in Hydrol. Earth Syst. Sci. Discuss.: 23 May 2016
Revised: 30 October 2016 – Accepted: 14 November 2016 – Published: 9 December 2016

Abstract. The Budyko functions $B_1(\Phi_p)$ are dimensionless relationships relating the ratio E/P (actual evaporation over precipitation) to the aridity index $\Phi_p = E_p/P$ (potential evaporation over precipitation). They are valid at catchment scale with E_p generally defined by Penman's equation. The complementary evaporation (CE) relationship stipulates that a decreasing actual evaporation enhances potential evaporation through the drying power of the air which becomes higher. The Turc–Mezentsev function with its shape parameter λ, chosen as example among various Budyko functions, is matched with the CE relationship, implemented through a generalised form of the advection–aridity model. First, we show that there is a functional dependence between the Budyko curve and the drying power of the air. Then, we examine the case where potential evaporation is calculated by means of a Priestley–Taylor type equation (E_0) with a varying coefficient α_0. Matching the CE relationship with the Budyko function leads to a new transcendental form of the Budyko function $B_1{}'(\Phi_0)$ linking E/P to $\Phi_0 = E_0/P$. For the two functions $B_1(\Phi_p)$ and $B_1{}'(\Phi_0)$ to be equivalent, the Priestley–Taylor coefficient α_0 should have a specified value as a function of the Turc–Mezentsev shape parameter and the aridity index. This functional relationship is specified and analysed.

1 Introduction

The Budyko curves are analytical formulations of the functional dependence of actual evaporation E on moisture availability, represented by precipitation P, and atmospheric water demand, represented by potential evaporation E_p. They are valid on long timescales at catchment scale. More precisely, the Budyko functions relate the evaporation fraction E/P to an aridity index defined as $\Phi_p = E_p/P$. Empirical formulations have been obtained by simple fitting to observed values (Turc, 1954; Budyko, 1974). Analytical derivations have also been developed (Mezentsev, 1955; Fu, 1981; Zhang et al., 2004; Yang et al., 2008). The Budyko relationships have been extensively used in the scientific literature up to now and interpreted with physical models (Gerrits et al., 2009) or thermodynamic approaches (Wang et al., 2015). For some of the formulations the shape of the curve is determined by a parameter linked to catchment characteristics such as vegetation, soil water storage (Li et al., 2013; Yang et al., 2007) or catchment slope (Yang et al., 2014). The most representative functions $E/P = B(\Phi_p)$ are shown in Table 1 (see Lebecherel et al., 2013 for an historical overview) and one of them (Turc–Mezentsev) is represented in Fig. 1 for different values of its shape parameter. All the Budyko functions assume steady-state conditions, which means that all the water consumed by evaporation comes from the precipitation and that the change in catchment water storage is nil: $P - E = Q$ with Q the total runoff. Consequently, the following conditions should be met: (i) $E = 0$ if $P = 0$, (ii) $E \leq P$ (water limit), (iii) $E \leq E_p$ (energy limit), (iv) $E \to E_p$ if $P \to +\infty$. These conditions define a physical domain where the Budyko curves are constrained (Fig. 1). It is worth noting that the Budyko functions, initially derived and used on long timescales, have been subsequently downscaled to the

Table 1. Different expressions of the Budyko functions as a function of the aridity index Φ_p.

Equation	Reference
$E/P = \left\{\Phi_p \tanh(\frac{1}{\Phi_p})\left[1-\exp\left(-\Phi_p\right)\right]\right\}^{1/2}$	Budyko (1974)
$E/P = \Phi_p\left[1+\left(\Phi_p\right)^{\lambda}\right]^{-\frac{1}{\lambda}}$	Turc (1954) with $\lambda = 2$, Mezentsev (1955), Yang et al. (2008)
$E/P = 1+\Phi_p-\left[1+\left(\Phi_p\right)^{\omega}\right]^{\frac{1}{\omega}}$	Fu (1981), Zhang et al. (2004)
$E/P = \frac{1+w\Phi_p}{1+w\Phi_p+\Phi_p^{-1}}$	Zhang et al. (2001)
$E/P = \Phi_p\left(\frac{k}{1+k\Phi_p^n}\right)^{1/n}$	Zhou et al. (2015)

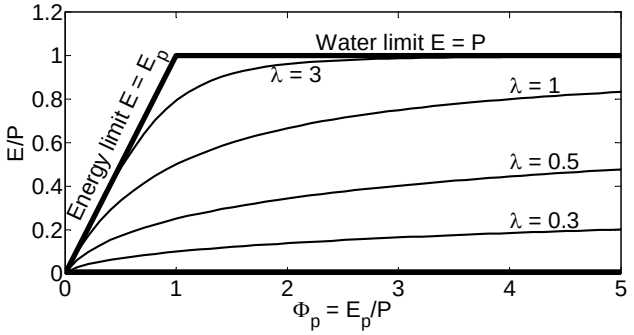

Figure 1. The Turc–Mezentsev relationship Eq. (4) between the ratio E/P and the aridity index $\Phi_p = E_p/P$ for four values of the parameter λ (0.3, 0.5, 1 and 3). The bold lines indicate the upper and lower limits of the feasible domain.

season or the month through analytical adjustments (Zhang et al., 2008; Du et al., 2016; Greve et al., 2016). It is interesting to note also that any Budyko function B_1 relating E/P to Φ_p can be transformed into a corresponding function B_2 relating E/E_p to $\Phi_p^{-1} = P/E_p$ (Zhang et al., 2004; Yang et al., 2008). Indeed we have:

$$\frac{E}{E_p} = B_2\left(\Phi_p^{-1}\right) = \frac{E}{P}\frac{P}{E_p} = B_1(\Phi_p)\Phi_p^{-1} = \Phi_p^{-1}B_1\left(\frac{1}{\Phi_p^{-1}}\right). \quad (1)$$

Potential evaporation establishes an upper limit to the evaporation process in a given environment. It is generally given by a Penman-type equation (Lhomme, 1997a), which is the sum of two terms – a first term depending on the radiation load R_n and a second term involving the drying power of the ambient atmosphere E_a:

$$E_p = \frac{\Delta}{\Delta+\gamma}R_n + \frac{\gamma}{\Delta+\gamma}E_a. \quad (2)$$

In Eq. (2) γ is the psychrometric constant and Δ the slope of the saturated vapour pressure curve at air temperature. E_a represents the capacity of the ambient air to extract water from the surface. It is an increasing function of the vapour pressure deficit of the air D_a and of wind speed u through a wind function $f(u)$: $E_a = f(u)D_a$. Contrary to precipitation, potential evaporation E_p is not a forcing variable independent of the surface. E_p is in fact coupled to E by means of a functional relationship known as the complementary evaporation (CE) relationship (Bouchet, 1963), which stipulates that potential evaporation increases when actual evaporation decreases. This complementary behaviour is made through the drying power of the air E_a: a decreasing actual evaporation makes the ambient air drier, which enhances E_a and thus potential evaporation. Equation (2) takes into account this complementary behaviour through the drying power E_a, which adjusts itself to the conditions generated by the rate of actual evaporation. It is also the case, for instance, when E_p is calculated as a function of pan evaporation. Observational data confirm that the CE relationship generally holds on daily to annual timescales (Morton, 1983; Lintner et al., 2015), which means that the matching between the two relationships (CE and Budyko) on long timescales is legitimate.

In most of the Budyko type functions encountered in the literature, potential evaporation E_p is generally not defined with accuracy. Choudhury (1999, p. 100) noted that "varied methods were used to calculate E_p, and these methods can give substantially different results". Moreover, in the original framework and in some subsequent works (e.g. Choudhury, 1999; Donohue et al., 2007), net radiation alone is used as a good approximation of the energy available for evaporation. Many formulae, in fact, can be used to calculate the potential rate of evaporation, each one involving different weather variables and yielding different values. Some formulae are based upon temperature alone, others on temperature and radiation (Carmona et al., 2016). In the present study we examine the case where E_p is estimated via a Priestley–Taylor type equation (Priestley and Taylor, 1972) with a variable co-

efficient α_0:

$$E_0 = \alpha_0 \frac{\Delta}{\Delta + \gamma} R_n. \quad (3)$$

Here, soil heat flux is neglected on large timescale and the coefficient α_0 (named the "Priestley–Taylor" coefficient) has not the fixed value (1.26) mentioned in the original work of Priestley–Taylor. It is supposed to increase with climate aridity and could vary from around 1.25 up to 1.75 according to Shuttleworth (2012). This can be seen as a direct consequence of the complementary evaporation relationship. Indeed, α_0 is linked to E_a by $\alpha_0 = 1 + (\gamma/\Delta)\, E_a/R_n$ (obtained by matching Eqs. 2 and 3), which shows that α_0 increases when the drying power rises. Lhomme (1997b) made a thorough examination of the so-defined coefficient α_0 by means of a convective boundary layer model.

In the present paper, the behaviour of the drying power of the air E_a will be examined, together with its physical boundaries, in relation to the actual rate of evaporation predicted by the Budyko functions. We will also show that the coefficient α_0, which allows an estimate of potential evaporation through the Priestley–Taylor equation (Eq. 3), has a functional relationship with the shape parameter of the Budyko curve and the aridity index, this last point constituting our main objective. Once α_0, and thus potential evaporation E_0, is determined, actual evaporation can be estimated either through the Budyko function or the CE relationship. The standpoint used in the study differs from various previous attempts undertaken in the literature to examine from different perspectives the links between Bouchet and Budyko relationships, investigating their apparent contradictory behaviour (Szilagyi and Jozsa, 2009). For example, Zhang et al. (2004) established a parallel between the assumptions underlying Fu's equation and the complementary relationship. In a study by Yang et al. (2006) concerning numerous catchments in China, the consistency between Bouchet, Penman and Budyko hypotheses was theoretically and empirically explained. Lintner et al. (2015) examined the Budyko and complementary relationships using an idealised prototype representing the physics of large-scale land–atmosphere coupling in order to evaluate the anthropogenic influences. Zhou et al. (2015) developed a complementary relationship for partial elasticities to generate Budyko functions, their relationship fundamentally differing from Bouchet's one. Carmona et al. (2016) proposed a power law to overcome a physical inconsistency of the Budyko curve in humid environments, this new scaling approach implicitly incorporating the complementary evaporation relationship.

The paper is organised as follows. First, the basic equations used in the development are detailed: the choice of a particular Budyko function is discussed and the complementary evaporation relationship, implemented through a generalised form of the advection–aridity model (Brutsaert and Stricker, 1979) is presented. Second, the feasible domain of the drying power of the air E_a is examined, together with its correspondence in dimensionless form with actual evaporation, as predicted by the Budyko function. Third, the functional relationship linking the Priestley–Taylor coefficient α_0 to the shape parameter of the Budyko function and the aridity index is inferred. In the following development, "complementary evaporation" is abbreviated to CE.

2 Basic equations

Among the Budyko functions given in Table 1, one particular form is retained in our study: the one initially obtained by Turc (1954) and Mezentsev (1955) through empirical considerations and then analytically derived by Yang et al. (2008) through the resolution of a Pfaffian differential equation with particular boundary conditions. Three reasons guided this choice: (i) the function is one of the most commonly used; (ii) it involves a model parameter λ which allows it to evolve within the Budyko physical domain; (iii) it has a notable simple mathematical property expressed as: $F(1/x) = F(x)/x$. This last property means that the same mathematical expression is valid for B_1 and B_2 (Eq. 1). The so-called Turc–Mezentsev function is expressed as:

$$\frac{E}{P} = B_1(\Phi_p) = \Phi_p \left[1 + (\Phi_p)^{\lambda}\right]^{-\frac{1}{\lambda}} = \left[1 + (\Phi_p)^{-\lambda}\right]^{-1/\lambda}. \quad (4)$$

It is written here with an exponent noted λ instead of the n generally used (Yang et al., 2009). The slope of the curve for $\Phi_p = 0$ is 1. When the model parameter λ increases from 0 to $+\infty$, the curves grow from the x axis (zero evaporation) to an upper limit (water and energy limits), as shown in Fig. 1. In other words, when λ increases, actual evaporation gets closer to its maximum rate and when Φ_p tends to infinite E/P tends to 1. The intrinsic property of Eq. (4) allows it to be transformed into a similar equation with E/E_p replacing E/P and Φ_p^{-1} replacing Φ_p (see Fig. 2a, b):

$$\frac{E}{E_p} = B_2\left(\Phi_p^{-1}\right) = \Phi_p^{-1}\left[1 + \left(\Phi_p^{-1}\right)^{\lambda}\right]^{-\frac{1}{\lambda}} = \left[1 + \left(\Phi_p^{-1}\right)^{-\lambda}\right]^{-1/\lambda}. \quad (5)$$

Fu (1981) and Zhang et al. (2004) derived a very similar equation with a shape parameter ω (see Table 1) and Yang et al. (2008) established a simple linear relationship between the two parameters ($\omega = \lambda + 0.72$). In the rest of the paper, the development and calculations are made with the Turc–Mezentsev formulation. However, similar (but less straightforward) results can be obtained with the Fu–Zhang formulation (see Sect. 4 in the Supplement).

The complementary evaporation (CE) relationship expresses that actual evaporation E and potential evaporation E_p are related in a complementary way following:

$$E_p + bE = (1 + b)E_w. \quad (6)$$

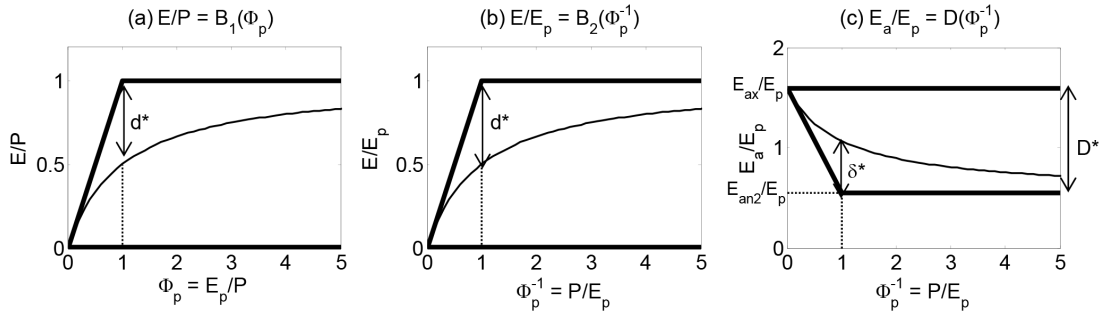

Figure 2. Correspondence between the two forms of the Turc–Mezentsev functions ($E/P = B_1(\Phi_p)$ and $E/E_p = B_2(\Phi_p^{-1})$ given by Eqs. 4 and 5) and the function defining the drying power of the air ($E_a/E_p = D(\Phi_p^{-1})$ given by Eq. 10). The calculations are made with $b = 1$, $\lambda = 1$ and a temperature of 15 °C: $d^* = 0.50$, $D^* = 1.05$ and $\delta^* = 0.52$. The bold lines indicate the limits of the feasible domain.

E_w is the wet environment evaporation, which occurs when $E = E_p$ and $b \geq 1$ is a proportionality coefficient which accounts for the asymmetry of the relationship (Han et al., 2012): the increase in potential evaporation is generally higher than the reduction in actual evaporation. Various forms of the CE relationship exist in the literature (Xu et al., 2005; Brutsaert, 2015; Szilagyi et al., 2016) and the value of b has been largely discussed (Kahler and Brutsaert, 2006; Pettijohn and Salvucci, 2009; Aminzadeh et al., 2016). In our analysis, the CE relationship is interpreted in the widely accepted framework of the advection–aridity model (Brutsaert and Stricker, 1979), where b is assumed to be equal to 1, potential evaporation E_p is calculated using Penman's equation (Eq. 2) and E_w is expressed by the original Priestley–Taylor equation with a fixed value (1.26) of the coefficient α_w:

$$E_w = \alpha_w \frac{\Delta}{\Delta + \gamma} R_n. \tag{7}$$

E_w only depends on net radiation and air temperature through Δ. The value of α_w has been the subject of discussion (Mallick et al., 2013): its analytical expression inferred from a land–atmosphere coupling model by Lintner et al. (2015) tends to prove that it could be lower than 1.26, in line with the in situ observations of Kahler and Brutsaert (2006). The value of 1.26, nevertheless, is kept in our numerical simulations, together with the value of 1 for b. All the algebraic calculations, however, will be performed with non-prescribed values of b and α_w, which allows other possible numerical simulations.

At this stage of the development it is important to make clear that two different Priestley–Taylor coefficients are defined in our analysis in relation to the CE relationship: one (α_w) is used to define the wet environment evaporation E_w and the other (α_0) to calculate the potential evaporation E_0, which is a substitute for the "true" potential evaporation E_p represented by Penman's equation (Eq. 2). E_0 (Eq. 3) being a substitute for E_p, it should also verify the CE relationship (Eq. 6), which implies that: $\alpha_w \leq \alpha_0 \leq (1+b)\alpha_w$. As already said in the introduction, the complementarity between E and E_p is essentially made through the drying power of the air E_a: a decrease in regional actual evaporation, consecutive to a decrease in water availability, generates a drier air, which enhances E_a and thus E_p. The behaviour of E_a is examined in the next section.

3 Feasible domain of the drying power of the air and correspondence with the evaporation rate

As a consequence of land–atmosphere interactions expressed by the CE relationship, the drying power of the air E_a is linked to the evaporation rate. Its feasible domain is examined hereafter by determining its bounding frontiers and its behaviour is assessed as a function of the evaporation rate. Inverting Eq. (2) and replacing its radiative term by E_w (Eq. 7) yields:

$$E_a = \left(1 + \frac{\Delta}{\gamma}\right)\left(E_p - \frac{E_w}{\alpha_w}\right). \tag{8}$$

Taking into account the CE relationship (Eq. 6) and scaling by E_p leads to:

$$\frac{E_a}{E_p} = \left(1 + \frac{\Delta}{\gamma}\right)\left[1 - \frac{1}{(1+b)\alpha_w}\left(1 + b\frac{E}{E_p}\right)\right]. \tag{9}$$

Inserting Eq. (5) into Eq. (9) gives:

$$\frac{E_a}{E_p} = D\left(\Phi_p^{-1}\right) = \left(1 + \frac{\Delta}{\gamma}\right) \left(1 - \frac{1}{(1+b)\alpha_w}\left\{1 + b\Phi_p^{-1}\left[1 + \left(\Phi_p^{-1}\right)^{\lambda}\right]^{-\frac{1}{\lambda}}\right\}\right). \tag{10}$$

This means that the ratio E_a/E_p can be also expressed and drawn as a function of Φ_p^{-1} like the Budyko functions. Given that there is a water limit expressed by $0 < E < P$ and an energy limit expressed by $0 < E < E_p$, the function $E_a/E_p = D(\Phi_p^{-1})$ should meet the following three conditions:

i. $E > 0$ implies that $E_a < E_{a,x}$ given by:

$$\frac{E_{a,x}}{E_P} = \left(1+\frac{\Delta}{\gamma}\right)\left[1-\frac{1}{(1+b)\alpha_w}\right]. \quad (11)$$

ii. $E < P$ implies that $E_a > E_{a,n1}$ given by:

$$\frac{E_{a,n1}}{E_p} = \left(1+\frac{\Delta}{\gamma}\right)\left[1-\frac{1}{(1+b)\alpha_w}\left(1+b\frac{P}{E_P}\right)\right]. \quad (12)$$

iii. $E < E_p$ implies that $E_a > E_{a,n2}$ given by:

$$\frac{E_{a,n2}}{E_p} = \left(1+\frac{\Delta}{\gamma}\right)\left(1-\frac{1}{\alpha_w}\right). \quad (13)$$

With E_p as scaling parameter, the feasible domain of E_a/E_p in the dimensionless space ($\Phi_p^{-1} = P/E_p$, E_a/E_p) is shown in Fig. 2c with $b = 1$: when evaporation is nil, $E_a = E_{a,x}$ is maximum (upper boundary in Fig. 2c); when evaporation is maximal, E_a is minimal (lower boundary in Fig. 2c). The maximum dimensionless difference D^* between the upper boundary ($E_{a,x}/E_p$) and the lower boundary is obtained by subtracting Eq. (13) from Eq. (11):

$$D^* = \frac{b}{(1+b)\alpha_w}\left(1+\frac{\Delta}{\gamma}\right). \quad (14)$$

There is a correspondence between the Budyko curves $E/P = B_1(\Phi_p)$ and $E/E_p = B_2(\Phi_p^{-1})$ drawn into Fig. 2a, b and the one of $E_a/E_p = D(\Phi_p^{-1})$ drawn in Fig. 2c. Figure 2a, b, and c show this correspondence for a particular case defined by $b = 1$, $\lambda = 1$ and $\Delta = 110\,\mathrm{Pa\,°C^{-1}}$ ($T = 15\,°C$). When the Budyko curves reach their upper limit, i.e. in very evaporative environments, the corresponding curve E_a/E_p reaches its lower limit. Conversely, when the Budyko curves reach their lower limit, i.e. the x axis (non-evaporative environment), the corresponding E_a/E_p curve reaches its upper limit.

It is interesting to note that the shape parameter λ of the Turc–Mezentsev function has a clear graphical expression. Indeed, denoting by d^* the maximum difference between the Turc–Mezentsev curve and its upper limit (Fig. 2a), this difference ($0 < d^* < 1$) obviously occurring for $\Phi_p = P/E_p = 1$, we have from Eq. (4):

$$d^* = 1 - 2^{-\frac{1}{\lambda}}, \quad (15)$$

which leads to:

$$\lambda = \frac{-\ln 2}{\ln(1-d^*)}. \quad (16)$$

When d^* varies from 1 to 0, the parameter λ varies from 0 to $+\infty$. The value corresponding to d^* in the graphical representation of $E_a/E_p = D(\Phi_p^{-1})$ (Fig. 2c) is the difference δ^* between the E_a/E_p curve (Eq. 10) and its lower boundary (Eq. 13) for $\Phi_p^{-1} = P/E_p = 1$. It is given by

$$\delta^* = \left(1+\frac{\Delta}{\gamma}\right)\frac{b}{(1+b)\alpha_w}\left(1-2^{-\frac{1}{\lambda}}\right) = D^* d^*. \quad (17)$$

This simple relationship shows that the dimensionless differences d^* and δ^* vary simultaneously in the same direction with a proportionality coefficient equal to D^*, whose value is close to 1. It is a direct consequence of the CE relationship. When d^* decreases, i.e. the dimensionless evaporation rate (E/P or E/E_p) increases, δ^* decreases, i.e. the drying power of the air E_a decreases: the air becomes wetter (assuming a constant wind speed). In the next section, another consequence of the CE relationship will be examined in relation to the value of the Priestley–Taylor coefficient α_0 and its dependence on the rate of actual evaporation.

4 Linking the Priestley–Taylor coefficient to the Budyko functions

Using the CE relationship as a basis, this section examines the link existing between the Priestley–Taylor coefficient α_0 defined by Eq. (3) and the Turc–Mezentsev shape parameter λ (Eq. 4). Combining Eqs. (3), (6) and (7) potential evaporation can be written as:

$$E_p = (1+b)\frac{\alpha_w}{\alpha_0}E_0 - bE. \quad (18)$$

Substituting E_p in Eq. (4) by its value given by Eq. (18) and putting $\Phi_0 = E_0/P$ gives

$$\frac{E}{P} = \left[\frac{(1+b)\alpha_w}{\alpha_0}\Phi_0 - b\frac{E}{P}\right]\left\{1+\left[\frac{(1+b)\alpha_w}{\alpha_0}\Phi_0 - b\frac{E}{P}\right]^{\lambda}\right\}^{-1/\lambda}. \quad (19)$$

Equation (19) can be rewritten as:

$$\Phi_0 = {B_1}'^{-1}\left(\frac{E}{P}\right) = \frac{\alpha_0}{(1+b)\alpha_w}\left\{\left[\left(\frac{E}{P}\right)^{-\lambda} - 1\right]^{-1/\lambda} + b\frac{E}{P}\right\}. \quad (20)$$

Equation (20) represents a transcendental form of the Turc–Mezentsev function (Eq. 4) issued from the complementary relationship and written with $\Phi_0 = E_0/P$ instead of $\Phi_p = E_p/P$. Calling ${B_1}'$ this new function $E/P = {B_1}'(\Phi_0)$, Eq. (20) represents in fact its inverse function $\Phi_0 = {B_1}'^{-1}(E/P)$. The function $E/P = {B_1}'(\Phi_0)$ has properties similar to the Turc–Mezentsev function (Eq. 4) (see the demonstrations in Sect. S1): (i) when Φ_0 tends to zero, ${B_1}'(\Phi_0)$ tends to zero with a slope equal to $\alpha_w/\alpha_0 (\leq 1)$; (ii) when Φ_0 tends to infinite, E/P tends to 1. A transcendental form of Eq. (5), called ${B_2}'$, can be obtained by expressing E/E_0 as a function of $\Phi_0^{-1} = P/E_0$:

$$\Phi_0^{-1} = {B_2}'^{-1}\left(\frac{E}{E_0}\right)$$

$$= \left\{ \left(\frac{E}{E_0} \right)^{-\lambda} - \left[\frac{(1+b)\alpha_w}{\alpha_0} - b \frac{E}{E_0} \right]^{-\lambda} \right\}^{-1/\lambda}. \quad (21)$$

Function $B_2{}'$ has the following properties at its limits (see Sect. S2): (i) when Φ_0^{-1} tends to zero, $B_2{}'(\Phi_0^{-1})$ tends to zero with a slope equal to 1; (ii) when Φ_0^{-1} tends to infinite, E/E_0 tends to $\alpha_w/\alpha_0 (\leq 1)$. For a given value of the exponent λ and fixed values of α_0 and $\alpha_w (= 1.26)$, the relationship between E/P and Φ_0 (or between E/E_0 and Φ_0^{-1}) can be obtained by numerically solving Eqs. (20) and (21). Similar calculations, more or less complicated, could be made with any Budyko function (Table 1). These results show that a Turc–Mezentsev curve (or any Budyko curve) generates a different curve when potential evaporation is given by E_0 instead of E_p. The new curve $B_1{}'$ is represented in Fig. 3a by comparison with the original one B_1 for two values of the shape parameter λ (0.5 and 2) and $b = 1$, assuming $\alpha_0 = \alpha_w = 1.26$. The new curve has a form similar to the original one, with the same limits at 0 and $+\infty$, but it is higher or lower depending on the value of α_0. In Fig. 3b the two curves are drawn when α_0 is adjusted according to Eq. (22) to make same closer. It is worth noting also that $B_2{}'$ is different from $B_1{}'$, contrary to B_2 (Eq. 5) which is identical to B_1 (Eq. 4), but the two curves are very close, as shown in Fig. 4, and it is easy to verify they have the same value for $\Phi_0 = \Phi_0^{-1} = 1$.

We have now two sets of Budyko functions: B'_1 and B'_2 (Eqs. 20, 21) involving $\Phi_0 = E_0/P$ and their corresponding original formulations B_1 and B_2 (Eqs. 4, 5) as a function of $\Phi_p = E_p/P$. The question now is to find out the value of α_0 which allows B'_1 to be equivalent (or the closest) to the original Turc–Mezentsev function B_1. Both equations expressing E/P as a function of an aridity index Φ (Φ_p or Φ_0), the expression of α_0 can be inferred by matching Eqs. (20) and (4): for a given value of the aridity index Φ, B_1 and $B_1{}'$ should give the same value of E/P. This leads to:

$$\alpha_0 = \frac{(1+b)\alpha_w}{1 + b\left(1+\Phi^{\lambda}\right)^{-1/\lambda}}. \quad (22)$$

The same relationship (Eq. 22) is obtained by matching B'_2 with B_2. Putting the value of α_0 defined by Eq. (22) into $B_1{}'$ and $B_2{}'$ (Eqs. 20, 21) leads to new transcendental equations linking E/P and Φ_0 (or E/E_0 and Φ_0^{-1}) which are exactly equivalent to the original Turc–Mezentsev functions (Eqs. 4, 5). Function $B_1{}'$ transforms into:

$$\frac{E}{P} + \left[\left(\frac{E}{P} \right)^{-\lambda} - 1 \right]^{-1/\lambda} = \Phi_0 + \left(1 + \Phi_0^{-\lambda} \right)^{-1/\lambda}, \quad (23)$$

and $B_2{}'$ into:

$$\left\{ 1 + \left[1 + \left(\Phi_0^{-1} \right)^{-\lambda} \right]^{-1/\lambda} - \frac{E}{E_0} \right\}^{-\lambda} = \left(\frac{E}{E_0} \right)^{-\lambda} - \left(\Phi_0^{-1} \right)^{-\lambda}. \quad (24)$$

In Sect. S3 we show that the original Turc–Mezentsev functions are the solutions of these transcendental equations. It

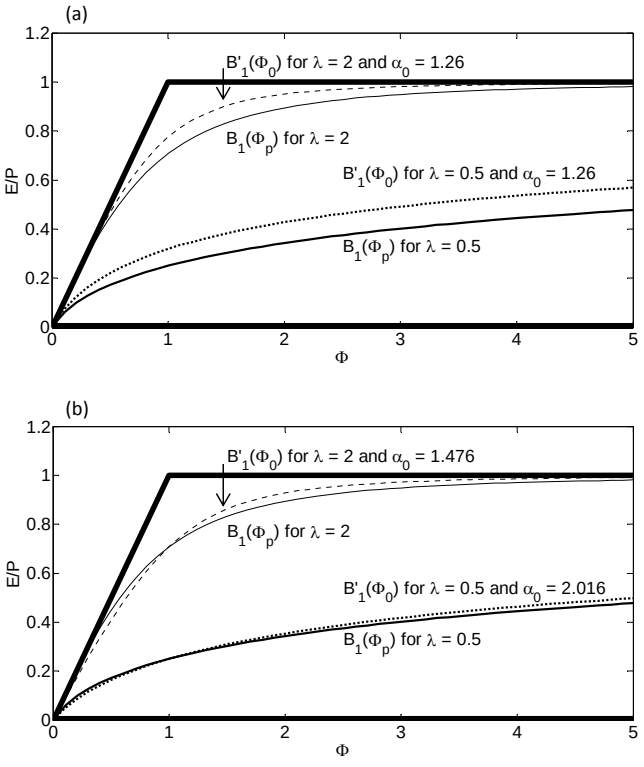

Figure 3. Comparison between the Turc–Mezentsev function $B_1(\Phi_p)$ (Eq. 4) in solid line and its corresponding function $B_1{}'(\Phi_0)$ (Eq. 20) in dotted line for two values of λ (0.5 and 2) and $b = 1$: **(a)** with $\alpha_0 = \alpha_w = 1.26$; **(b)** with α_0 adjusted according to Eq. (22) for $\Phi = 1$. The x axis legend Φ represents either Φ_p for $B_1(\Phi_p)$ or Φ_0 for $B_1{}'(\Phi_0)$.

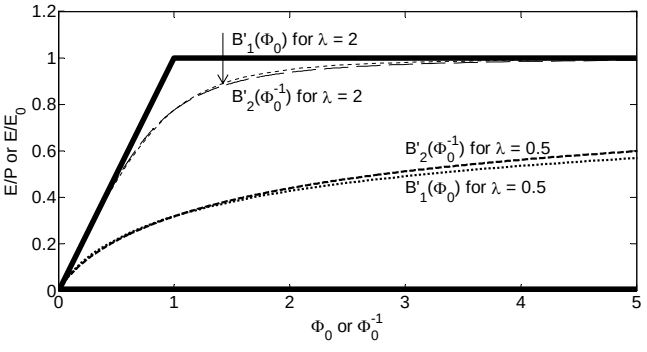

Figure 4. Comparison of functions $E/P = B_1{}'(\Phi_0)$ (Eq. 20) and $E/E_0 = B_2{}'(\Phi_0^{-1})$ (Eq. 21) for two different values of the shape parameter λ (0.5 and 2), $b = 1$ and $\alpha_0 = 1.26$.

is also worth noting that when α_0 is expressed by Eq. (22) and Φ_0 tends to zero (or Φ_0^{-1} tends to infinite), α_w/α_0 in Eqs. (20) and (21) tends to 1. This means that these equations have the same limits as their original equations (Eqs. 4, 5).

For every value of λ and Φ, a unique value of α_0 can be calculated by means of Eq. (22), b and α_w being fixed. In this equation $\alpha_0 = f(\lambda, \Phi)$, Φ represents climate aridity and

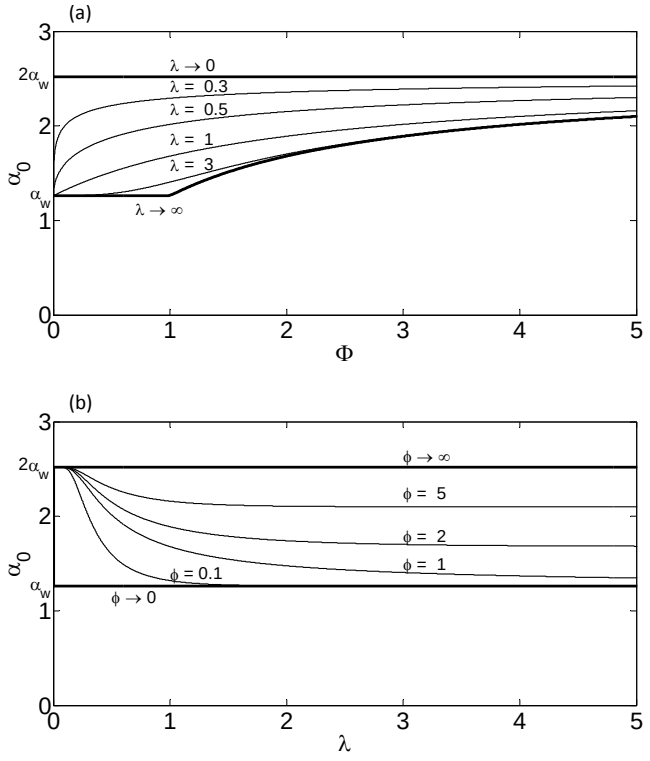

Figure 5. Variation of the Priestley–Taylor coefficient α_0 (Eq. 22 with $b = 1$ and $\alpha_w = 1.26$): **(a)** as a function of the aridity index Φ for different values of the shape parameter λ of the Turc–Mezentsev function; **(b)** as a function of λ for different values of the aridity index Φ. The bold lines indicate the limits of the feasible domain.

λ represents the catchment characteristics in relation to its ability to evaporate (the greater λ, the higher its evaporation capability). The Priestley–Taylor coefficient α_0 appears to be an increasing function of Φ and a decreasing function of λ. Figure 5a shows the relationship between α_0 and λ for different values of Φ: when λ tends to zero (non-evaporative catchment), α_0 tends to $(1+b)\alpha_w = 2\alpha_w$, whatever the value of Φ. When λ tends to infinity (i.e. very evaporative catchment), the limit of α_0 depends on the value of Φ: for $\Phi \leq 1$ the limit is α_w and for $\Phi > 1$ the limit is the branch of the hyperbole $(1+b)\alpha_w\Phi/(b+\Phi) = 2\alpha_w\Phi/(1+\Phi)$. Figure 5b shows the relationship between α_0 and Φ for different values of λ. When Φ tends to $+\infty$ (very arid catchment), the coefficient α_0 tends to $(1+b)\alpha_w = 2\alpha_w$. When Φ tends to 0 (very humid catchment), α_0 tends to α_w. These results illustrate the simple functional relationship existing between the Priestley–Taylor coefficient, the Budyko shape parameter and the aridity index. Very similar results are obtained when the Fu–Zhang formulation is used instead of the Turc–Mezentsev one, as detailed in Sect. S4. In the last Sect. S5, Fig. 5a, b are redrawn with a value of $b = 4.5$, as obtained by Brutsaert (2015) from a reformulated complementary relationship. The general shape of the curves is very similar, but the upper limits are much higher in agreement with a higher value of b.

5 Summary and conclusion

The Budyko curves have two different and equivalent dimensionless expressions: B_1 where E/P is a function of the aridity index $\Phi_p = E_p/P$, and B_2 where E/E_p is a function of $\Phi_p^{-1} = P/E_p$; any B_1 curve can be transformed into an equivalent B_2 curve and vice versa. Among various Budyko type curves, the Turc–Mezentsev one (Eq. 4) with the shape parameter λ was chosen because it is commonly used and has the remarkable property of having the same mathematical expression in both representations B_1 or B_2. Using Penman's equation (Eq. 2) to express potential evaporation and introducing the complementary evaporation relationship in the form of the advection–aridity model with its parameters b and α_w (Eqs. 6, 7), it was shown that the dimensionless drying power of the air $D = E_a/E_p$ expressed as a function of Φ_p^{-1} has upper and lower boundaries and that there is a functional correspondence between the Budyko and D curves. Next, we examined the case where potential evaporation is expressed by the Priestley–Taylor equation (E_0 given by Eq. 3) with a varying coefficient α_0 instead of the sounder Penman's equation. Introducing the advection–aridity model shows that the Turc–Mezentsev function linking E/P to $\Phi_p = E_p/P$ (Eq. 4) transforms into a new transcendental form of the Budyko function $B_1{}'$ linking E/P to $\Phi_0 = E_0/P$ (Eq. 20), only numerically resolvable. The Priestley–Taylor coefficient α_0 should have a specified value as a function of b, α_w, λ and $\Phi_0 = \Phi_p$ so that the two curves B_1 and $B_1{}'$ be equivalent. This means that the coefficient α_0 with $\alpha_w \leq \alpha_0 \leq (1+b)\alpha_w$ is intrinsically linked to the shape parameter λ of the Turc–Mezentsev function and to the aridity index.

List of symbols

B_1	function linking E/P to $\Phi_p = E_p/P$
$B_1{}'$	function linking E/P to $\Phi_0 = E_0/P$ given by Eq. (20)
B_2	function linking E/E_p to $\Phi_p^{-1} = P/E_p$
$B_2{}'$	function linking E/E_0 to $\Phi_0^{-1} = P/E_0$ given by Eq. (21)
b	asymmetry coefficient of the CE relationship (Eq. 6)
D	function linking E_a/E_p to P/E_p
D^*	difference between the upper and lower boundaries of D (–)
d^*	maximum difference between the Budyko curve and its upper limit (–)
E	actual evaporation (LT^{-1})
E_p	potential evaporation expressed by Penman's equation (Eq. 2) (LT^{-1})
E_0	potential evaporation expressed by the Priestley–Taylor equation (Eq. 3) (LT^{-1})
E_w	wet environment evaporation in the CE relationship (Eq. 7) (LT^{-1})

E_a	drying power of the air (LT^{-1})
$E_{a,n1}$	lower limit of E_a given by Eq. (12) (LT^{-1})
$E_{a,n2}$	lower limit of E_a given by Eq. (13) (LT^{-1})
$E_{a,x}$	upper limit of E_a given by Eq. (11) (LT^{-1})
P	precipitation (LT^{-1})
R_n	net radiation (LT^{-1})
α_0	varying coefficient of the Priestley–Taylor equation E_0 (–)
α_w	$= 1.26$ fixed coefficient of the Priestley–Taylor equation E_w (–)
γ	psychrometric constant ($ML^{-1}T^{-2}{}^\circ C^{-1}$)
Δ	slope of the saturated vapour pressure curve at air temperature ($L^{-1}T^{-2}{}^\circ C^{-1}$)
δ^*	maximum difference between the E_a/E_p curve and its lower boundary (–)
λ	shape parameter of the Turc–Mezentsev equation ($\lambda > 0$) (–)
Φ_0	aridity index calculated with $E_0 (\Phi_0 = E_0/P)$ (–)
Φ_p	aridity index calculated with $E_p (\Phi_p = E_p/P)$ (–)

The Supplement related to this article is available online at doi:10.5194/hess-20-4857-2016-supplement.

Acknowledgements. The authors are very grateful to three anonymous reviewers and the handling editor for their constructive comments. They also gratefully acknowledge the UMR LISAH for its valuable scientific support and significant financial contribution, as well as A. Gaby for having inspired some of the main ideas of the paper.

Edited by: F. Tian
Reviewed by: three anonymous referees

References

Aminzadeh, M., Roderick, M. L., and Or, D.: A generalized complementary relationship between actual and potential evaporation defined by a reference surface temperature, Water Resour. Res., 52, 385–406, doi:10.1002/2015WR017969, 2016.

Bouchet, R.: Evapotranspiration réelle et potentielle, signification climatique, IAHS Publ., 62, 134–142, 1963 (in French).

Brutsaert, W.: A generalized complementary principle with physical constraints for land-surface evaporation, Water Resour. Res., 51, 8087–8093, doi:10.1002/2015WR017720, 2015.

Brutsaert, W. and Stricker, H.: An advection-aridity approach to estimate actual regional evapotranspiration, Water Resour. Res., 15, 443–450, 1979.

Budyko, M. I.: Climate and life, Academic Press, Orlando, FL, 508 pp., 1974.

Carmona, A. M., Poveda, G., Sivapalan, M., Vallejo-Bernal, S. M., and Bustamante, E.: A scaling approach to Budyko's framework and the complementary relationship of evapotranspiration in humid environments: case study of the Amazon River basin, Hydrol. Earth Syst. Sci., 20, 589–603, doi:10.5194/hess-20-589-2016, 2016.

Choudhury, B. J.: Evaluation of an empirical equation for annual evaporation using field observations and results from a biophysical model, J. Hydrol., 216, 99–110, doi:10.1016/S0022-1694(98)00293-5, 1999.

Donohue, R. J., Roderick, M. L., and McVicar, T. R.: On the importance of including vegetation dynamics in Budyko's hydrological model, Hydrol. Earth Syst. Sci., 11, 983–995, doi:10.5194/hess-11-983-2007, 2007.

Du, C., Sun, F., Yu, J., Liu, X., and Chen, Y.: New interpretation of the role of water balance in an extended Budyko hypothesis in arid regions, Hydrol. Earth Syst. Sci., 20, 393–409, doi:10.5194/hess-20-393-2016, 2016.

Fu, B. P.: On the calculation of evaporation from land surface, Sci. Atmos. Sin., 5, 23–31, 1981 (in Chinese).

Gerrits, A. M. J., Savenije, H. H. G., Veling, E. J. M., and Pfister, L.: Analytical derivation of the Budyko curve based on rainfall characteristics and a simple evaporation model, Water Resour. Res., 45, W04403, doi:10.1029/2008WR007308, 2009.

Greve, P., Gudmundsson, L., Orlowsky, B., and Seneviratne, S. I.: A two-parameter Budyko function to represent conditions under which evapotranspiration exceeds precipitation, Hydrol. Earth Syst. Sci., 20, 2195–2205, doi:10.5194/hess-20-2195-2016, 2016.

Han, S., Hu, H., and Tian, F.: A nonlinear function approach for the normalized complementary relationship evaporation model, Hydrol. Process., 26, 3973–3981, doi: 10.1002/hyp.8414, 2012.

Kahler, D. M. and Brutsaert, W.: Complementary relationship between daily evaporation in the environment and pan evaporation, Water Resour. Res., 42, W05413, doi:10.1029/2005WR004541, 2006.

Lebecherel, L., Andréassian, V., and Perrin, C.: On regionalizing the Turc–Mezentsev water balance formula, Water Resour. Res., 49, 7508–7517, doi:10.1002/2013WR013575, 2013.

Lhomme, J.-P.: Towards a rational definition of potential evaporation, Hydrol. Earth Syst. Sci., 1, 257–264, doi:10.5194/hess-1-257-1997, 1997a.

Lhomme, J.-P.: An examination of the Priestley–Taylor equation using a convective boundary layer model, Water Resour. Res., 33, 2571–2578, 1997b.

Li, D., Pan, M., Cong, Z., Zhang, L., and Wood, E.: Vegetation control on water and energy balance within the Budyko framework, Water Resour. Res., 49, 969–976, doi:10.1002/wrcr.20107, 2013.

Lintner, B. R., Gentine, P., Findell, K. L., and Salvucci, G. D.: The Budyko and complementary relationships in an idealized model of large-scale land–atmosphere coupling, Hydrol. Earth Syst. Sci., 19, 2119–2131, doi:10.5194/hess-19-2119-2015, 2015.

Mallick, K., Jarvis, A., Fisher, J. B., Tu, K. P., Boegh, E., and Niyogi, D.: Latent heat flux and canopy conductance based on Penman-Monteith, Priestley–Taylor equation, and Bouchet's complementary hypothesis, J. Hydrometeor., 14, 419–442, doi:10.1175/JHM-D-12-0117.1, 2013.

Mezentsev, V.: More on the computation of total evaporation, Meteorol. Gidrol., 5, 24–26, 1955 (in Russian).

Morton, F. I.: Operational estimates of areal evapotranspiration and their significance to the science and practice of hydrology, J. Hydrol., 66, 1–76, 1983.

Pettijohn, J. C. and Salvucci, G. D.: A new two-dimensional physical basis for the complementary relation between terrestrial and pan evaporation, J. Hydrometeorol., 10, 565–574, doi:10.1175/2008JHM1026.1, 2009.

Priestley, C. H. B. and Taylor, R. J.: On the assessment of surface heat flux and evaporation using large-scale parameters, Mon. Weather Rev., 100, 81–92, 1972.

Shuttleworth, W. J.: Terrestrial hydrometeorology, Wiley-Blackwell, UK, 448 pp., 2012.

Szilagyi, J. and Jozsa, J.: Complementary relationship of evaporation and the mean annual water-energy balance, Water Resour. Res., 45, W09201, doi:10.1029/2009WR008129, 2009.

Szilagyi, J., Crago, R., and Qualls, R. J.: Testing the generalized complementary relationship of evaporation with continental-scale long-term water-balance data, J. Hydrol., 540, 914–922, doi:10.1016/j.jhydrol.2016.07.001, 2016.

Turc, L.: Le bilan d'eau des sols: relations entre les précipitations, l'évaporation et l'écoulement, Ann. Agron., Série A(5), 491–595, 1954.

Wang, D., Zhao, J., Tang, Y., and Sivapalan, M.: A thermodynamic interpretation of Budyko and L'vovich formulations of annual water balance: proportionality hypothesis and maximum entropy production, Water Resour. Res., 51, 3007–3016, doi:10.1002/2014WR016857, 2015.

Xu, C. Y. and Singh, V. P.: Evaluation of three complementary relationship evapotranspiration models by water balance approach to estimate actual regional evapotranspiration in different climatic regions, J. Hydrol., 308, 105–121, doi:10.1016/j.jhydrol.2004.10.024, 2005.

Yang, D., Sun, F., Liu, Z., Cong, Z., and Lei, Z.: Interpreting the complementary relationship in non-humid environments based on the Budyko and Penman hypotheses, Geophys. Res. Lett., 33, L18402, doi:10.1029/2006GL027657, 2006.

Yang, D., Sun, F., Liu, Z., Cong, Z., Ni, G., and Lei, Z.: Analyzing spatial and temporal variability of annual water-energy balance in nonhumid regions of China using the Budyko hypothesis, Water Resour. Res., 43, W04426, doi:10.1029/2006WR005224, 2007.

Yang, D., Shao, W., Yeh, P. J. F., Yang, H., Kanae, S., and Oki, T.: Impact of vegetation coverage on regional water balance in the nonhumid regions of China, Water Resour. Res., 45, W00A14, doi:10.1029/2008WR006948, 2009.

Yang, H., Yang, D., Lei, Z., and Sun, F.: New analytical derivation of the mean annual water-energy balance equation, Water Resour. Res., 44, W03410, doi:10.1029/2007WR006135, 2008.

Yang, H., Qi, J., Xu, X., Yang, D., and Lv, H.: The regional variation in climate elasticity and climate contribution to runoff across China, J. Hydrol., 517, 607–616, doi:10.1016/j.jhydrol.2014.05.062, 2014.

Zhang, L., Hickel, K., Dawes, W. R., Chiew, F. H. S., Western, A. W., and Briggs, P. R.: A rational function approach for estimating mean annual evapotranspiration, Water Resour. Res., 40, W02502, doi:10.1029/2003WR002710, 2004.

Zhang, L., Potter, N., Hickel, K., Zhang, Y., and Shao, Q.: Water balance modeling over variable time scales based on the Budyko framework – Model development and testing, J. Hydrol., 360, 117–131, doi:10.1016/j.jhydrol.2008.07.021, 2008.

Zhou, S., Yu, B., Huang, Y., and Wang, G.: The complementary relationship and generation of the Budyko functions, Geophys. Res. Lett., 42, 1781–1790, doi:10.1002/2015GL063511, 2015.